Photorefractive self-defocusing

Mordechai Segev, Yoav Ophir, and Baruch Fischer
Department of Electrical Engineering, Technion—Israel Institute of Technology, Haifa 32 000, Israel

(Received 3 October 1989; accepted for publication 15 January 1990)

Self-defocusing of a Gaussian light beam in a bulk photorefractive $BaTiO_3$ crystal is demonstrated. This is a low light intensity process which results from the coupling and power transfer between the spatial frequency components of the beam. We use this effect in photorefractive waveguide structure for all-optical switching with very low light powers.

Self-focusing of light beams is a well known phenomenon in nonlinear optics.[1,2] It is caused by the self-modification of the index of refraction by the optical field via Kerr-like effects, and requires relatively high-power densities of light. Nonlinear photorefractivity also exhibits a behavior of self-index modification but of a different nature. It is based on charge separation in the material by light excitation, diffusion, or drift of electrons or holes which are retrapped in a nonuniform spatial distribution according to the light intensity. The space-charge field induces index of refraction changes which are almost independent of the absolute light intensity (down to $\mu W/cm^2$) but only on the spatial variations. The Fanning effect,[3,4] for example, is an asymmetric self-scattering process in photorefractive media. It results from scattered light by imperfections which is amplified in a broad-angle region. Recently, we have reported[5] on nonlinear mode-coupling effects in photorefractive waveguides. In the funnel-like process the low-order modes are amplified by the high-order ones, and the opposite high mode amplification occurs in the antifunneling process.

In this letter we present an experimental demonstration of photorefractive self-defocusing of a Gaussian beam that propagates along the c axis of a $BaTiO_3$ crystal. The effect is achievable with very low light intensities of a few mW/cm^2. It is based on a funneling-like process[5] in which the high spatial frequencies of the beam amplify the low frequencies via photorefractive nonlinear beam coupling. The analysis of this process, as well as the opposite process of self-focusing in photorefractive materials, is given. We emphasize that these effects do not originate from noise amplification as they do in the Fanning effect.

In the experiment we used a poled $BaTiO_3$ crystal with dimensions of $5\times5\times5$ mm^3. A spatially filtered and linearly polarized Gaussian beam of the argon ion laser's 515.5 nm line was inputed into the crystal by an objective with a numerical aperture of 0.3. The waist at the focus was about 1 μm. The propagation direction was along the crystal's c axis. Figure 1(a) shows the result of the self-defocusing effect. A circular spot size of the input beam turns into a noncircular elongated shape. According to the analysis below, it is caused by a transversal spatial frequency collapse. In that process, the low frequencies are amplified in the transverse axis which is parallel to the polarization direction [the horizontal direction in Fig. 1(a) or the y axis in the analysis]. The photorefractive coupling is very strong in that direction (which makes the polarization extraordinary), and is negligible in the perpendicular one (ordinary polarization). A rotation of the polarization direction evokes the strong coupling in the new (extraordinary) polarization direction and causes a similar rotation of the elongated cross-section output as shown in Fig. 1(b) for a rotation of 90°.

A theoretical analysis of the process can be carried out according to Refs. 5 and 6. The paraxial propagating beam is represented by its plane wave components or its transverse spatial frequencies $\bar{q}\equiv(q_x,q_y)$. The transverse plane is denoted by $\bar{r}\equiv(x,y)$. The coupled equations for these plane wave components, in the usual approximations of slowly varying amplitudes and negligible absorption, are given by[6]

$$\frac{d\tilde{F}(\bar{q},z)}{dz}=\frac{1}{F_0}\int_{-\infty}^{\infty}\Gamma(\bar{q},\bar{q}')\tilde{F}(\bar{q},z)\tilde{F}(\bar{q}',z)dq_x'\,dq_y', \quad (1)$$

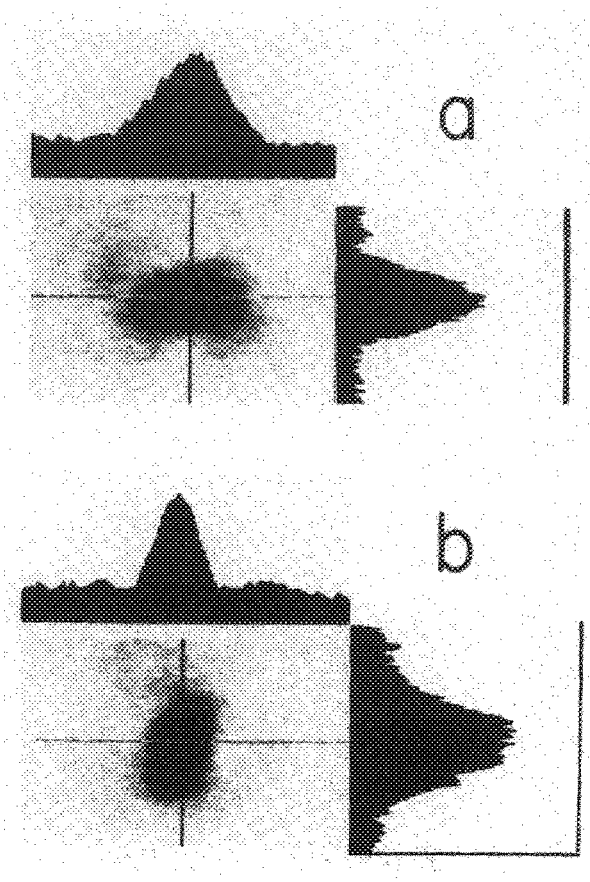

FIG. 1. Self-defocusing experimental output showing the cross section of the beam with (a) horizontal polarization. Here the vertical direction is unaffected by the photorefractive nonlinear coupling. (b) For vertical beam polarization the picture is rotated by 90°.

 0003-6951/90/121086-03$02.00

where

$$\tilde{F}(\bar{q},z) = F(\bar{q},z)\cos\alpha,$$

$$F(\bar{q},z) = \left| \int_{-\infty}^{\infty} A(\bar{r}) e^{-i\bar{q}\cdot\bar{r}} dx\, dy \right|^2,$$

$$F_0 = \int_{-\infty}^{\infty} F(\bar{q},z)\, dq_x\, dq_y,$$

and $A(\bar{r})$ is the beam amplitude. α and α_0 are the angles with the z direction (the c axis) of the corresponding plane wave component and the mean propagation directions ($\alpha_0 = 0$ in our experiment). Then, $\sin(\alpha - \alpha_0) = (\lambda/2\pi)q, (q = |\bar{q}|)$, λ is the wavelength, and

$$\Gamma(\bar{q},\bar{q}') = -\Gamma(\bar{q}',\bar{q}) = (1/\cos\alpha\cos\alpha')2\,\mathrm{Re}\,\gamma(\bar{q},\bar{q}'). \tag{2}$$

γ is the coupling parameter given by[5–7]

$$\gamma(\bar{q},\bar{q}') = -\left[i\omega r_{\mathrm{eff}}(\bar{q},\bar{q}')n_0^3/2c\right]E_m(\bar{q},\bar{q}'). \tag{3}$$

E_m, which is proportional to the space-charge field and the effective electro-optic coefficient r_{eff} depends on the geometry, polarizations, and material parameters. In our photorefractive crystal, the coupling constant is very strong in the polarization direction (along the y axis) of the beam and negligible in the perpendicular one.[5] This makes the difference between the two transversal directions and gives the noncircular elongated output. This also enables the approximation in the next paragraph, in which we restricted our numerical calculation to $\bar{q}$ in the polarization direction (y axis) and solved the one-dimensional problem.

The numerical solution of Eq. (1) was carried out for coupling in one dimension (q_y), using a computer program for nonlinear coupled equations. We have divided the angular range of q_y for the interacting beams to small intervals, each representing a plane wave component. The calculation is similar for mode coupling in photorefractive waveguides,[5] where each mode can be represented by two plane waves having opposite angles α and $-\alpha$ with the propagation direction. We have also used the $BaTiO_3$ crystal parameters from Ref. 5, with a beam propagation along the symmetry c axis to construct the matrix of the coupling constants,

$$\Gamma = \begin{pmatrix} A & B \\ B & A \end{pmatrix}. \tag{4}$$

The beam components were ordered according to their angles (spatial frequencies), starting from $q_y = 0$ to higher positive angles, followed by increasing negative angles from $q_y = 0$. Then A and B are antisymmetric. A represents coupling of beam components with the same sign for q_y while B contains coupling constants for components with opposite signs. We also note that in our geometry and notation $\Gamma(q_y,q_y') = \Gamma(-q_y,-q_y')$, all A_{ij} and B_{ij} elements have the same sign (positive or negative) for $j > i(|q_y'| > |q_y|)$ and an opposite sign for elements with $j < i$ (corresponding to $|q_y'| < |q_y|$). The positive sign case gives the funneling process in which the high $|i|$ spatial frequencies are converted into the low ones. The antifunneling process occurs for the negative sign case, obtainable by an opposite beam propagation.

The funneling process in the spatial frequencies space gives a self-defocusing effect in the real transversal space, and the antifunneling causes self-focusing. The central column in Fig. 2 shows the effect of the coupling where the beam propagates 0.5 cm along the positive direction of the c axis. We can see the funneling and the corresponding self-defocusing behavior. Self-focusing and antifunneling occur for opposite beam propagation. The input (output) in the self-focusing example can serve as the output (input) in the self-defocusing and funneling case. In the calculation we have decomposed the input Gaussian beam into its spatial frequency Fourier components $[F(q_y)]$ in the y direction. Equation (4) was then used to obtain the nonlinear interaction effect in the frequency space. The output in the real space (upper part of Fig. 2) is the inverse transform (lower part), which gives the transversal y dependence of the field. Not surprisingly, the exact Gaussian structure is not preserved. The right column of Fig. 2 shows the opposite self-focusing (and antifunneling) process where the beam propagation and the coupling constants have opposite direction and signs. It is important to note that we have neglected in our calculations any phase changes in the beam spatial frequency components. Linear phase changes due to free propagation are negligible in short distances of a few millimeters, and there is no contribution of nonlinear phases in diffusion-dominated photorefractive wave mixing (where γ_{ij} is real[4]). We should note that adding noise to the calculation did not change the results significantly. In the Fanning effect, however, the noise was found to be very important.[6] Another factor that minimizes the noise amplification is the small cross section of the input beam.[4]

Figure 3 shows the evolution of the spatial frequency beam components as they propagate along the photorefractive medium. A wide frequency distribution of a Gaussian input gradually turns into a sharp peaked distribution around the zero spatial frequency. This is the funneling process.[5] For coupling constants with opposite signs (obtaina-

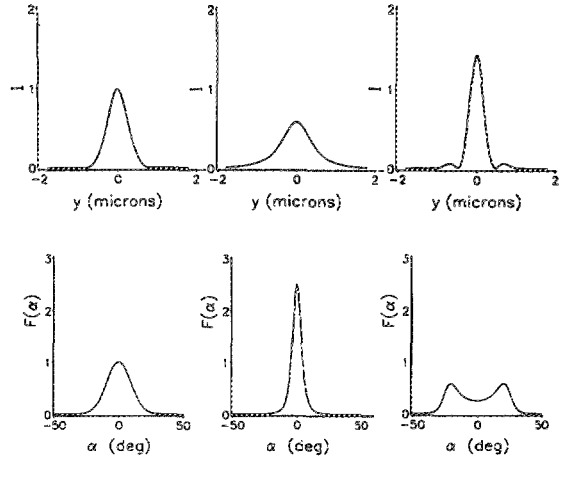

FIG. 2. Calculated self-focusing and self-defocusing of a Gaussian input beam that propagates 0.5 cm along the negative (for focusing) and positive (for defocusing) directions of the c axis. The left column shows the input beam as a function of y (upper) and its spatial frequencies (lower). The self-defocused output and its corresponding spatial frequency distribution (showing the funneling behavior) is given in the central column. The right figures show the self-focused output case. The spatial frequencies are given in terms of angles as described in the letter.

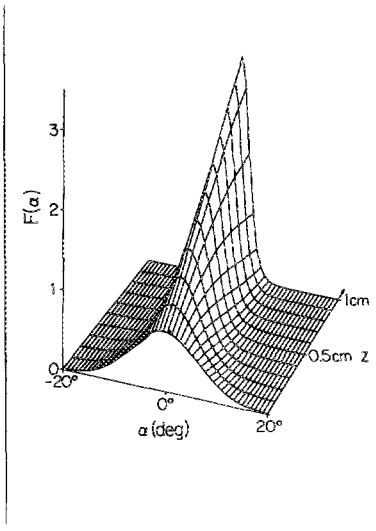

FIG. 3. Calculated evolution of a Gaussian input beam that propagates 1 cm along the c axis showing the funneling process as a function of the interaction length. The spatial frequencies are given in terms of angles as described in the letter.

ble in $BaTiO_3$ for opposite beam propagation), a reversed scenario of antifunneling occurs. Here the intensity of the low spatial frequencies decreases, while the high orders are amplified. We can obtain any prerequested degree of funneling (or antifunneling) into the low (high) spatial frequencies (with any small width δq_y around zero) for long enough interaction lengths $[z \gg z_0(\delta)]$, and

$$\lim_{z\to\infty,\delta q_y\to 0}\int_{-\delta q_y/2}^{\delta q_y/2} F(q_y)\,dq_y = F_0. \tag{5}$$

For the opposite propagation along the $-c$ direction, the antifunneling for very long interaction distance results in a collapse into a backward propagating wave. It is a different type of backscattering from the stimulated effect of Chang and Hellwarth.[8] In their case a phase conjugate reflection is produced by a huge amplification of noise due to the long collimated path of an input beam. Geometrical restriction maximizes the gain for backward noise for input directions which are not necessarily along the $-c$ axis.

As discussed in Ref. 1, the factor $1/F_0$ in Eq. (1) makes the effects dependent only on relative intensities of the wave components distribution, but not on the overall intensity. (It does affect the time response of the coupling.[7]) We also note that we can control the beam coupling, and hence the output, in several ways. Examples are illumination of the crystal by an incoherent background, applying an electric field, or changing the orientation and geometry of the crystal and the beam. From Eq. (1) we see that the coupling depends on the combined factor $(\Gamma z/F_0)$. Thus, changing F_0 by increasing

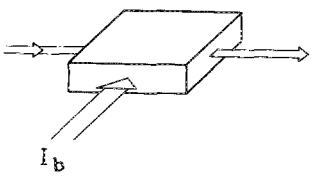

FIG. 4. Schematic of the experiment in which a background beam I_b controls the beam funneling in a photorefractive slab.

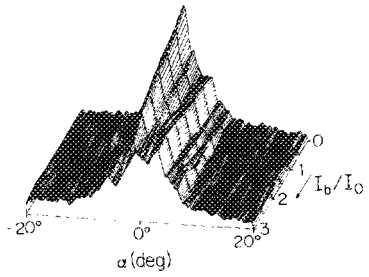

FIG. 5. Experimental output from the photorefractive slab showing the far-field structure as a function of the background light intensity I_b. It is similar to the dependence on $1/z$ in Fig. 3 of the output spatial frequency (or mode) distribution in the theoretical calculation.

the background light is equivalent to a change of Γ or the interaction length.

We have carried out an experiment showing the effect of background light. Instead of a bulk we have used a slab of a photorefractive 70-μm-thick and 5-mm-long $BaTiO_3$ crystal. It allows the use of a long interaction length with very effective nonlinear coupling. A high multimode input beam propagated along its c axis. Its power was about 60 μW. The strong funneling process[5] causes the collapse of all the modes into the low ones. The background light beam was shined into the slab from its side, as shown in Fig. 4, and deteriorated the coupling due to the increase of F_0. Figure 5 shows the experimental output as a function of the background light with powers of tens of μW. This behavior is similar to the theoretically calculated $1/z$ (or $1/\Gamma$) dependence of Fig. 3, as discussed above. We can use this feature to optically switch a light beam that passes the photorefractive slab with very low powers. The collapse into the low-order modes of the high multimode input beam by the strong funneling process, provides a maximum light power for a detector at the center. The control light beam deteriorates the coupling and makes the output unfunnelled and scattered in all of the modes. Now the detector measures low light power. In our experiment, the maximum power of the control beam was 180 μW, as shown in Fig. 5.

In conclusion, we have demonstrated the self-defocusing effect in the photorefractive $BaTiO_3$ crystal. An analysis of self-defocusing and self-focusing was given on the basis of photorefractive nonlinear multi-two-wave mixing. We have shown the effect of a background light illumination and used it for an all-optical switching device.

This work was supported by the Foundation for Research in Electronics, Computers and Communications, administrated by the Israel Academy of Science and Humanities and by the M&D Frocht Fund for Research.

[1] R. Y. Chiao, E. Garmire, and C. H. Townes, Phys. Rev. Lett. **13**, 479 (1964).
[2] P. L. Kelley, Phys. Rev. Lett. **15**, 1005 (1965).
[3] V. V. Voronov, I. R. Dorosh, Yu. S. Kuz'minov, and N. V. Tkachenko, Sov. J. Quantum Electron. **10**, 1346 (1981).
[4] G. Zhang, Q. X. Li, P. P. Ho, Z. K. Wu, and R. R. Alfano, Appl. Opt. **25**, 2955 (1986).
[5] B. Fischer and M. Segev, Appl. Phys. Lett. **54**, 684 (1989).
[6] M. Segev, Y. Ophir, and B. Fischer (unpublished).
[7] B. Fischer, S. Sternklar, and S. Weiss, IEEE J. Quantum Electron. **QE-25**, 550 (1989).
[8] T. Y. Zhang and R. W. Hellwarth, Opt. Lett. **10**, 408 (1985).